Proceedings of the 1st Global Power and Propulsion Forum
GPPF 2017
Jan 16-18, 2017, Zurich, Switzerland
www.pps.global

GPPF-2017-56

UNDERSTANDING, DESIGNING, AND INITIAL TESTING OF SMALL-SCALE HORIZONTAL AXIS WIND TURBINES FOR THE URBAN ENVIRONMENT

Kenneth W. Van Treuren
Baylor University
Kenneth_Van_Treuren@baylor.edu
Waco, TX, USA

Andrew Hays
Baylor University
Andrew_Hays@baylor.edu
Waco, TX, USA

ABSTRACT

Wind turbines are leading the generation of renewable energy. A long overlooked category of wind turbines is the small-scale wind turbine, the majority of which are horizontal axis wind turbines (HAWTs). New construction of buildings in cities are requiring some portion of the electrical power consumed by the building be generated by the building itself. In addition, an important topic of interest in the urban environment is the generation of noise. This paper describes the recent rise in the use of small-scale wind turbines and discusses the design of HAWTs for the urban environment. Also presented in this paper is the development and initial validation of a small-scale HAWT test stand for use in a small (0.61m X 0.61m cross-section) university research wind tunnel. This testing process can help with the design of new urban wind turbines by being able to use both geometric and Reynolds number scaling. The test stand developed can also study wind turbine noise and lead to modifications of the wind turbine blades to minimize noise production while at the same time seeking to optimize power output. Keywords: small-scale wind turbine, urban wind turbine, low Reynolds number wind turbine, and wind turbine noise.

INTRODUCTION

World population has reached over 7 billion people. Approximately 6 billion of these people live in developing countries, with nearly 84% living in rural areas. The United Nations projects the world population to grow to 9.7 billion people by the year 2050 [1]. In 2013, over 1.2 billion people, approximately 17% of the world's population, did not have access to electricity. World energy consumption is forecast to increase by 33% between 2013 and 2040 [2]. It is important that an adequate supply of energy be available for economic, cultural, and societal development. A vital component for providing a sustainable energy supply is wind energy. Wind Energy is the fastest growing renewable energy source, growing at approximately 2.9% per year. In fact, wind energy is responsible for 33% of the recent increase in renewable energy [3]. Wind energy grew substantially in 2015 [4]. New installations exceeded 63 GW, a 22% increase from 2014. This brings the total wind power worldwide to 433 GW. Wind power provided more new power generation in 2015 than any other technology. Currently more than 80 countries have wind energy with eight having more than 10 GW. In 2015, China led the way adding 30.8 GW (145 GW total), the United States was second adding 8.6 GW (76 GW total), and Germany was third with 3.78 GW added (45 GW total). Factors leading to these trends are the low cost of energy prices and continued favourable economic policies by countries towards adding new wind projects.

A category of wind energy often overlooked is that of small-scale wind turbines. The definition of small-scale can vary depending on geographic location [5-9]. Many definitions use rated power with the American Wind Energy Association defining any wind turbine producing less than 100 kW as small. Some use diameter and still others, such as the International Electrotechnical Commission, use a rotor swept area of 200 m^2, which equates to approximately 50 kW. Of particular interest to many applications are the small-scale wind turbine sub-categories of small, 0-1.5 kW, and micro, 1.5 kW–50 kW. Small-scale wind turbines saw 806,000 registered turbines worldwide in 2015 [5]. This category is forecast to grow at 20% per year to the year 2020. The growth is predominantly in China (72% of the installed market, 40% of capacity), the United States (18% of the installed market, 30 % of capacity), and the United Kingdom (3% of the installed market, 15% of capacity). Small wind is a cost effective way of generating electricity on the local level, both in remote settings as well as in conjunction with a national grid.

Small wind turbines work well as part of a grid network. Distributed wind is defined by the project's location relative to the end-use and power distribution infrastructure rather than the turbine or project size [10]. In the United States, 49% (capacity basis) of the documented 2015 distributed wind projects were connected to distribution lines serving local loads [10]. Using a distributed grid has its advantages. Micro-grids allow small communities to support themselves by

securing “island” micro-grids that can be disconnected from the main grid [11]. This makes micro-grids less susceptible to cyber or terrorist attack. Much needs to be done to develop these micro-grids, along with associated storage capabilities, to further enhance their potential. In the end, micro-grids provide less risk and a stronger, stable, and safer energy portfolio. This is an ideal scenario for urban wind turbines. Cities tend to consume 75% of all generated power [12] so it is only natural to generate power where people live. Buildings can be used to generate electricity with the goal of being a net zero energy building [13]. Countries such as France and Germany mandate incorporation of renewable energy production into new building construction. France and Sweden will have ‘net zero energy’ in all new buildings by 2020 [14]. Companies such as Aerotecture International Inc. design wind turbines specifically for the urban setting to be used on flat rooftops [15]. Micro-turbines lend themselves to clustering for increased power production in urban settings [16].

This paper will focus on understanding, designing, and testing of small-scale horizontal axis wind turbines for the urban environment. It is important to determine the correct performance of the wind turbine system model in order to both geometrically scale the wind turbine and to determine its predicted performance using Reynolds matching. Selection of an appropriate airfoil is essential for improved performance. The selection process for the airfoils, the design and fabrication of the blades, and the testing of the small-scale wind turbine system in a wind tunnel are discussed. A wind turbine test stand is developed to enable this testing of the wind turbine system in a small wind tunnel. The urban wind turbine will typically operate in a low Reynolds number environment so special care is given to the experimental testing which results in a wind turbine that will operate efficiently and quietly in the urban environment.

Urban Wind Turbines

A major advantage of small-scale wind turbines is the ability to produce power near the demand. Work is being done to harness the wind in major cities and convert this wind to electrical power [17]. As stated previously, cities consume an estimated 75% of all generated power [12]. Many suburban and residential areas do not have buildings at a sufficient height for meaningful energy production, but, in a larger city, skyscrapers can be used for energy production **[**18**]**. While the amount of energy that can be produced in an urban environment is much lower than that of open rural areas, it is still better to produce some power than no power at all [19]. Several studies have assessed the wind resources available on top of buildings and in densely packed urban environments [18, 20-22]. The main concern for an urban application when using a horizontal axis wind turbine is the variability of the flow direction and turbulence generated the surroundings. Surrounding structures can mix the flow, therefore, causing a challenging environment for the turbine. Studies have been done to estimate the potential for wind power in different urban environments and examining how the immediate and surrounding topography would affect the performance of a HAWT [23-25]. Some work has been done to design urban buildings for wind turbines and to enhance energy production [26]. By adding a wind turbine to a building or adding a building wind capture device for a turbine, the power density can be increased 3-8 times [27]. An example of using accelerated and captured flow with a building design is seen in Fig. 1. Assessing the potential of a specific turbine in an environment is also of major importance to determining the feasibility of wind power generation. Walker and Simic et al. both show that it is not the rated power but the power curve that defines the potential power generation [23, 29]. Due to the relatively low wind speeds in most urban environments, the cut-in speed and the rate at which the turbine reaches its maximum power potential are what will make a turbine feasible in an urban environment.

A major concern of wind turbines in urban environments is the noise produced [22]. While noise generation for large scale wind turbines and wind farms have been studied, these studies have not addressed small-scale turbines in the urban environment. With large turbines being removed from most residential areas, the noise levels for these large wind turbines are not of much concern. However, in a city or suburban neighborhood, the noise generated by a turbine can be substantial because of the higher RPMs required and, therefore, an annoyance. While some cities in the United States and smaller countries, such as New Zealand, have noise standards, there is no set standard across major borders or from different wind power associations as to what is an acceptable noise level. New Zealand, for example, states that the sound level at the boundary of any residential site must not exceed 40 dB or the background noise plus 5 dB [30]. When designing a wind turbine for the urban environment, noise generation must be a topic of interest. Design parameters include, and are not limited to, airfoil selection, rotational speed, tip speed ratio and tip designs. By addressing these and other parameters, an efficient and quiet urban wind turbine can be designed.

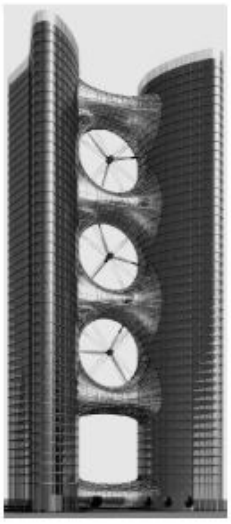

Figure 1. Urban Wind Turbine Design [28]

Types of Noise

The noise produced by an airfoil is widely recognized with six categories as defined by Brooks et al. [31]. These categories are further discussed by Wagner et al. [32] and are the categories used by the National Renewable Energy Laboratory (NREL) AirFoil Noise (NAFNoise) prediction tool [33]. These categories can be seen in Fig. 2. The six wind turbine noise categories are described by Van Treuren [34] as:

1. *Turbulent Boundary Layer-Trailing Edge Noise*: At higher Reynolds numbers turbulent boundary layers develop over much of the airfoil and the noise occurs as the turbulent eddies pass over the trailing edge. This is considered broadband noise in the range of 750 Hz < f <2 kHz. It is the main source of high-frequency noise, especially for medium and large wind turbines.
2. *Laminar Boundary Layer-Vortex Shedding Noise*: At lower Reynolds numbers a mostly laminar boundary layer develops over the blade and instabilities create a feedback loop of excited pressure waves. This leads to vortex shedding and its associated noise near the trailing edge. This type of airfoil noise is of interest for small-scale wind turbines at low Reynolds numbers. The noise is tonal and can be avoided with careful airfoil selection/design.
3. *Separation-Stall Noise*: This is noise due to a non-zero angle of attack of the wind turbine blade creating a boundary layer separation wake at the trailing edge. Very high angles of attack lead to large-scale separation (deep stall) at the trailing edge causing the airfoil to radiate low-frequency noise. At high angles the airfoil is acting similar to that of a bluff body in the flow. This also leads to broadband noise.
4. *Trailing Edge Bluntness Vortex Shedding Noise*: This is noise generated by a small separated region located at the blunt trailing edges of the turbine blade. This source is controlled by the shape of the trailing edge of the airfoil. This noise is considered tonal and can be avoided with careful design of the trailing edge.
5. *Tip Vortex Formation Noise*: This noise is created due to the vortices generated by flow at the tips of the turbine blades. This is considered broadband noise and is not fully understood.
6. *Turbulent Inflow Noise*: This is noise that is generated based on the incoming turbulence of the free stream air contacting the airfoil's leading edge which can influence all other noise categories. This contributes to broadband noise in the lower frequencies (250 Hz < f < 1000 Hz) but it is not yet fully quantified.

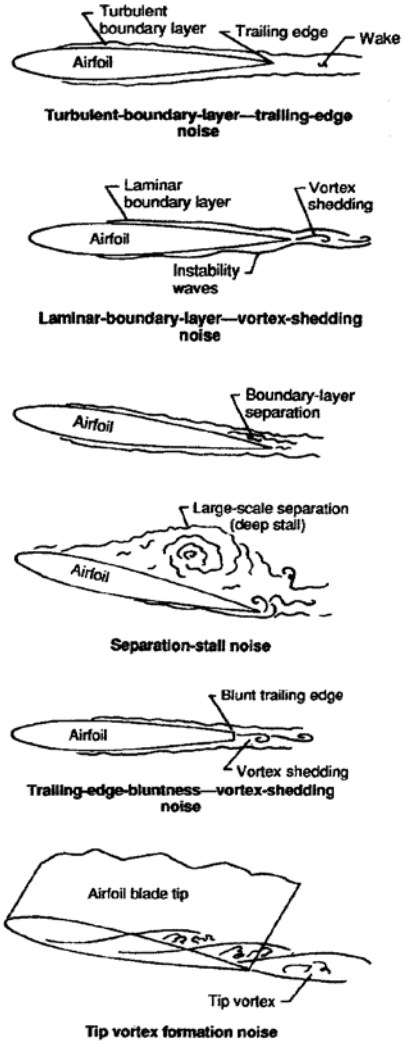

Figure 2. Types of Aeroacoustic Noise [31]

Airfoil Aerodynamics and Aeroacoustics

From previous studies done by Van Treuren and Hays [35, 36], airfoil selection is of utmost importance in the design of a small wind turbine when considering power production and noise generation. Other studies by Wisniewski et al. and Goçmen et al. further confirm that careful airfoil selection and design can make a significant difference in noise generation [37, 38]. From these studies, it was demonstrated airfoils with a thinner profile and increased camber can lower the noise generated by the airfoil.

Another factor of major importance with small-scale wind turbines is the low Reynolds numbers that occur over the blades. Due to slower wind speeds, approximately 5 m/s or less, coupled with smaller chord lengths, the Reynolds numbers are typically below 200,000. While there are several large databases of airfoils, such as the University of Illinois Urbana-Champaign [39], experimental data for low Reynolds number flows is very limited. Computational codes, such as XFOIL [40], exist and can provide accurate results for Reynolds numbers above 200,000. These codes do not accurately predict airfoil performance at lower Reynolds due to low momentum flow where separation can, and does occur. Experimental wind tunnel testing of airfoils at low Reynolds numbers is often necessary to accurately predict the aerodynamic performance. Previous studies by Van Treuren and Burdett et al. show that experimental testing is needed and the data can vary from computational predictions. Some of their results can be seen in Fig. 3 [41, 42].

With accurate, experimental aerodynamic data, a wind turbine blade can be designed for optimum power production

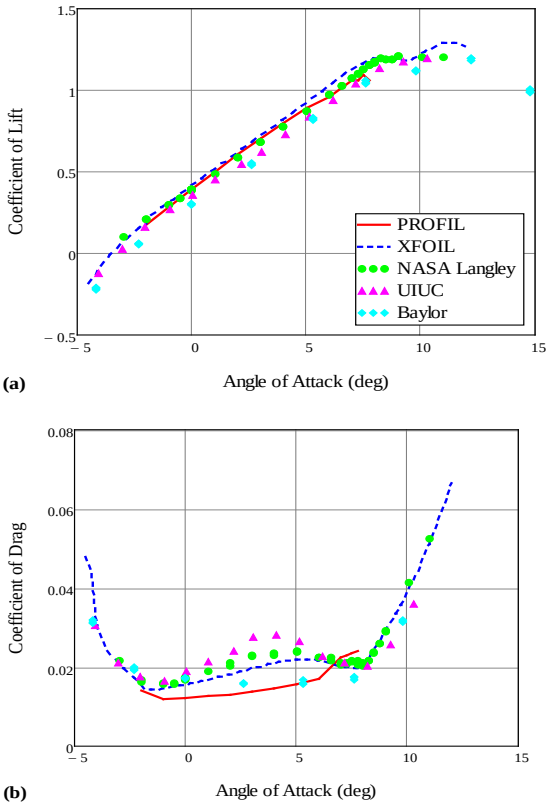

Figure 3. Eppler 387 Coefficient of (a) Lift and (b) Drag at a Reynolds Number of 100,000 [41, 42]

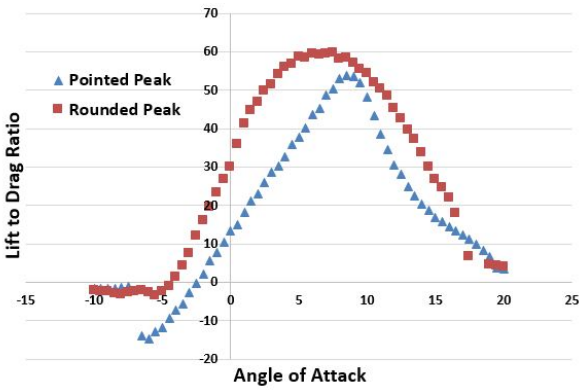

Figure 4. Lift to Drag Curves Compared [40]

based on the angle of attack for L/D_{MAX} of the airfoil selected. L/D_{MAX} is the angle which produces the most lift for the least amount of drag. This is where the most power will be produced. The L/D_{MAX} vs angle of attack curve shape is also very important for wind turbine design. A sharp peak implies that at an off-design operating condition near the design angle of attack, a loss of power production will occur. A plateaued or rounded peak shows that at an off-design operating condition, the losses will not be as significant. A comparison of these two types of curves is shown in Fig. 4. With an airfoil and an angle of attack chosen, a wind turbine blade can be designed.

Blade element momentum theory (BEMT) is commonly used to optimize a wind turbine blade for a specific tip speed

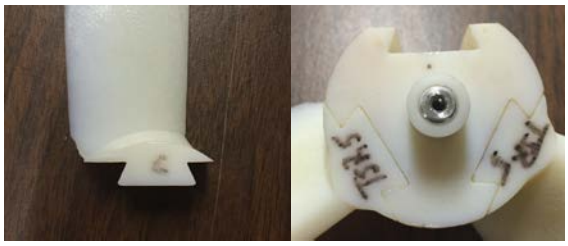

Figure 5. Dovetail Attachments

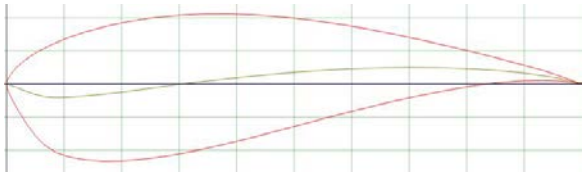

Figure 6. NREL S823 Airfoil [43]

Figure 7. Wind Turbine Blade

ratio (TSR) based on airfoil data and a desired chord length. A common TSR, and the one used for these tests, is five. With a blade designed, it can now be manufactured for testing. The blades used in these tests were fabricated with a rapid prototyping machine, an Objet 30 3-D printer. For the current study, each blade was printed individually with a dovetail attachment, which can be seen in Fig. 5. This allows for a method of rapidly changing blades for testing different configurations. With each blade manufactured, a hub and spinner were also printed to complete the wind turbine rotor. The airfoil chosen for previous studies by Burdett and used in these tests is the NREL S823 [43]. This airfoil is an NREL airfoil designed for low Reynolds number flow and used on small-scale wind turbines. The airfoil can be seen in Fig. 6. A wind turbine blade made from this airfoil using BEMT can be seen in Fig. 7.

Tip Treatments

As mentioned previously, tip vortices are a source of noise, and, due to the high rotational speeds of small wind turbines, this noise can be significant. Studies on small UAS propellers show that tip treatments on the blades significantly lower the noise signature of the propellers [37, 44]. While wind turbines are a different application, the aerodynamic principles remain the same and show promise for future small-scale wind turbines. All results presented in this paper were found using a square blade tip. Future studies will examine noise improvements by modifying the wind turbine blade tips.

Figure 8. Baylor Subsonic Wind Tunnel

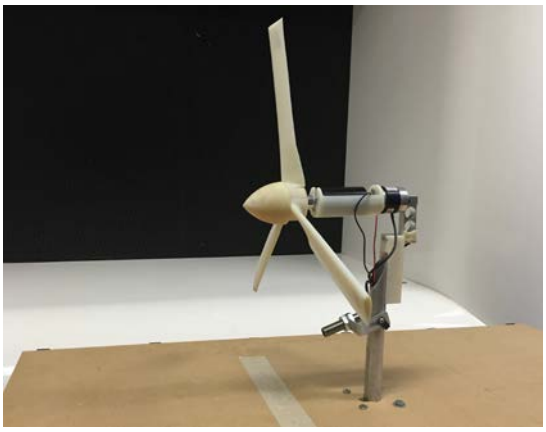

Figure 9. Wind Turbine Experimental Setup

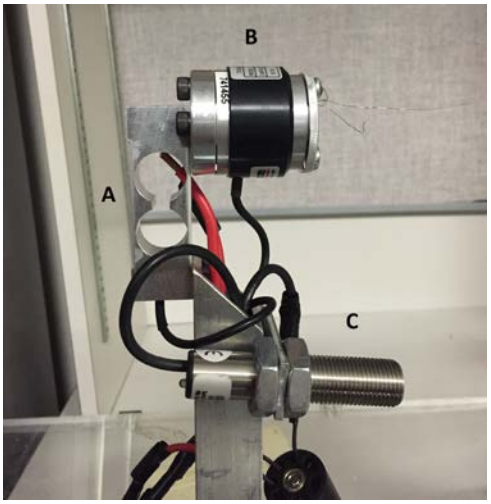

Figure 10. Load Transducer (a), Torque Transducer (b) and Optical Tachometer (c)

Development and Testing of a Wind Turbine Test Stand

Wind Tunnel

The wind turbine test stand was designed for use in the Baylor University (BU) Subsonic Wind Tunnel, seen in Fig. 8. The wind tunnel is an Engineering Laboratory Design, Inc. (ELD) Model 406B. This wind tunnel is open-circuit and has a constant-pitch fan driven by a variable-speed, 40-hp motor which allows wind speeds in the tunnel to range from 0.1-50 m/s (112 mph). The test section is 122 cm (48 in.) long with a 61 cm (24 in.) square cross section. With this test section, a 50.8 cm (20 in.) diameter wind turbine has been designed and tested. The turbine stand is centered in the tunnel test section and the plane of rotation is 40 cm (15.75 in.) from the test section entrance. The wind turbine experimental setup can be seen in Fig 9.

The cross-sectional area of the BU Subsonic Wind Tunnel test section is 0.372 m^2 (4 ft^2), and the rotor swept area of the turbine is 0.196 m^2 (2.113 ft^2), creating a blockage ratio of 52.8%. While this ratio is very high, previous work by Van Treuren and Burdett have validated testing small wind turbines of this size in the BU Subsonic Wind Tunnel [45]. Using the method described by Chen and Liou [46], they tested three wind turbines with different diameters, 0.5 m, 0.4 m, and 0.3 m with blockage ratios of 52.8%, 33.8%, and 19.0%, in the BU Subsonic Wind Tunnel, scaled both for Reynolds number and geometry. They showed that scaling and testing of wind turbines can be successfully accomplished in small wind tunnels, even with blockage ratios up to 52.8%.

Equipment and Calibration

A wind turbine test stand was developed to measure turbine rotor performance. The wind turbine rotor was connected to a Re-40 Maxon motor that was used as a generator. This generator is a graphite brushed motor with a power rating of 150 watts and a maximum efficiency of 92%. The horizontal thrust of the turbine was measured by an Interface LSP-1 thrust transducer. While thrust is measured and can be related to variables such as the axial induction factor, it is not used in the present analysis. The torque was measured by an Interface MRTP-0.2 Nm torque transducer. The torque value measured was used to calculate power production, one of three power calculation methods. These two transducers are seen in Fig. 10. The RPM of the turbine was measured with an Omega HHT20 optical tachometer, also seen in Fig. 10. The resistance load for the turbine was applied with a Clarostat Power Resistor Decade box. The voltage output of the generator was measured by a Newport TrueRMS voltmeter. With the resistance and voltage, a current value was calculated based on Ohm's Law. Using current and the manufacturer's torque constant for the generator, it is possible to calculate turbine power. This is a second method of finding the power generated. A third method is to calculate the actual power out of the system using the voltage and resistance. The velocity in the tunnel was measured by a pitot-static probe, which was attached to an Omega PCL-2A Differential Pressure Transducer. The velocity is needed to calculate the coefficient of power, C_p, of the wind turbine. The noise in the tunnel was measured by a Brüel & Kjaer Type 2670 ¼" microphone connected to a B&K 2270 Frequency Analyzer, seen in Fig. 11.

The transducers were connected to a National Instruments Compact DAQ system utilizing an NI 9205 DAQ-Card. With this system connected to a computer, the transducers were then

Figure 11. Brüel & Kjaer Microphone and Analyzer

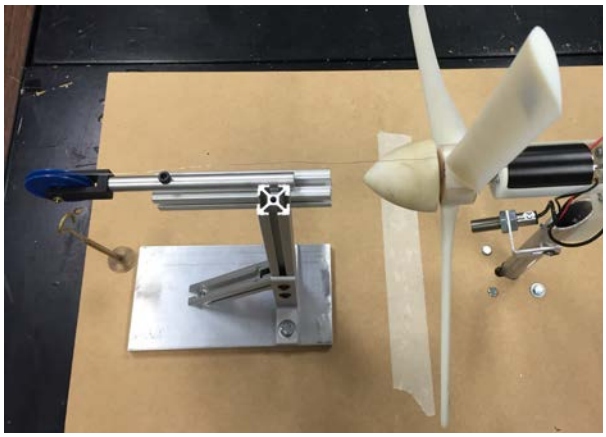

Figure 12. Thrust Calibration

Figure 13. Torque Calibration

read with a LabVIEW Virtual Instrument (VI). Sample rates were 5k Hz for five seconds.

Calibration of the thrust and torque transducers required a series of weights to be hung and the output voltages measured. The calibration of the thrust transducer can be seen in Fig. 12. The calibration of the torque transducer can be seen in Fig. 13. The calibration procedure for the Omega optical tachometer required the use of an ESL-20 Digital Stroboscope. The wind tunnel was run at different speeds and the RPM was measured using the stroboscope. The ¼" Brüel and Kjaer microphone used a Brüel and Kjaer Sound Calibrator.

Uncertainty Analysis

The Kline and McClintock method of uncertainty analysis was used to calculate the uncertainties in these experiments [47]. For all SPL measurements, the rated uncertainty of the B&K system is ±1.5 dB(A). For each set of C_P calculations, there was a different uncertainty value based on the calculation method for the coefficient. The torque transducer calculation of C_P had a total uncertainty of ±0.0272. The torque constant calculation of C_P had a total uncertainty of ±0.0147. The voltmeter calculation of C_P had a total uncertainty of ±0.0122. The uncertainty of the PCL-2A is ±0.0028 inches of water leading to an uncertainty in the velocity measured of ±0.00143 m/s. These results represent a sample calculation of the uncertainty at the maximum power point (MPP) with the tunnel speed at 5.59 m/s (12.5 mph).

Experimental Procedure

To begin testing, the wind turbine was inserted in to the tunnel along with the B&K microphone, which was set 31.75 cm (12.5 in.) downstream of the blades. This setup can be seen in Figure 14. The tunnel was run at 2.24, 3.35, 4.47, 5.59 and 6.71 m/s (5, 7.5, 10, 12.5, and 15 mph). Starting at 2.24 m/s (5 mph) and a resistance of 99 **Ω**, the resistance was reduced incrementally until the turbine stalled to find the MPP. When this was completed, the testing was repeated for each of the test speeds. A typical plot of C_p vs resistance can be seen in Fig. 15. Clearly from this plot, a MPP can be found for the given wind speed of 5.59 m/s (12.5 mph).

Once the MPP was found for each wind speed, the noise testing began. The B&K microphone was positioned 31.75 cm (12.5 in.) downstream of the blades and 2.5 cm (1 in.) above the tip of the turbine blade. Using the traverse system seen in Fig. 14, the microphone was moved downward towards the tunnel centreline. These noise measurements were completed for each wind speed.

Once noise testing was concluded, background noise was needed to correct the noise measurements of the wind turbine. To complete these tests, the turbine was taken out of the tunnel, and a clean floor was put in the test section. With this setup, the tunnel was empty except for the B&K microphone, which was then traversed to the same locations as the previous tests for each wind speed. With the background noise, a corrected A-weighted decibel level could be calculated. This calculation can be done using Eq. 1, seen below [48].

$$Noise_{\ Corrected} = 10 * (\log_{10}(10^{\frac{NoiseLevel}{10}} - 10^{\frac{CleanNoise}{10}})) \quad (1)$$

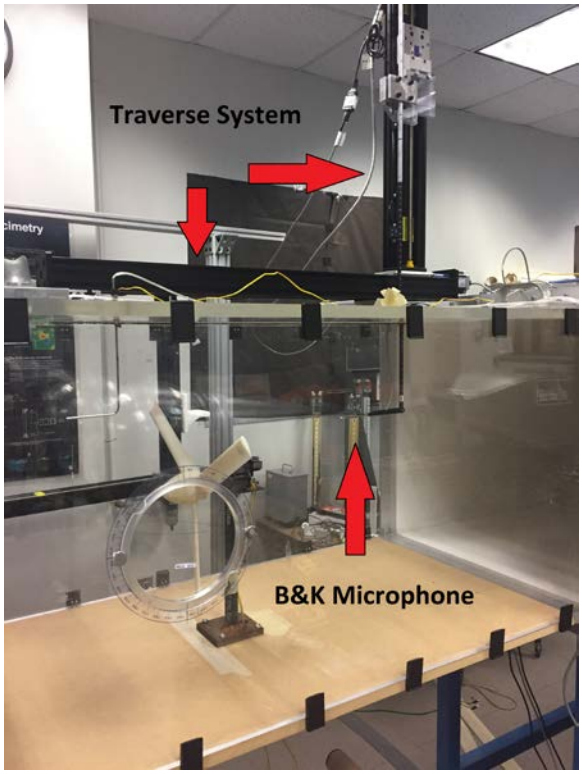

Figure 14. Wind Tunnel Test Section

Results

Figure 15 shows the coefficient of power versus resistance at 5.59 m/s (12.5 mph) for the three different measurement methods. The first calculates the power from the voltage and resistance measurements, the second calculates the power using the manufacturer supplied torque constant, and the third uses the torque measurement to calculate wind turbine power directly. From this graph, it is very evident that the change in resistance leads to a much higher coefficient of power, and, therefore, a higher power output. For the torque transducer this value was 21.1% C_p for a resistance of 7 Ω. Measuring the MPP shows that optimization for a desired wind speed is possible to produce maximum power.

Figure 16 shows the coefficient of power versus tip speed ratio for 5.59 m/s (12.5 mph). The wind turbine blades used in this test were optimized for a TSR of five, which can be clearly seen in the plot. The off-design TSRs show how much power loss can occur when operating off-design.

Figure 17 shows the coefficient of power versus wind speed, at the maximum power points. In this plot, as the wind speed increases, the coefficient of power increases as well.

With all three plots, it is very evident that for the three measurement methods, the voltmeter, the torque constant, and the torque transducer, all show similar results when calculating the coefficient of power. The voltmeter is consistently the lowest measurement because this takes in to account all the system losses. The generator is connected to the decade box, as is the voltmeter. The electrical losses of the generator, the decade box and the wires connecting these devices leads to a loss of power. The torque constant method depends on the manufacturer's data and is usually the center data value close to the torque transducer. The current used to

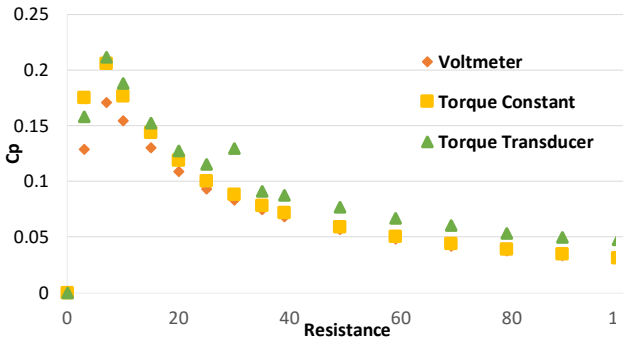

Figure 15. Coefficient of Power vs. Resistance at 5.59 m/s (12.5 mph)

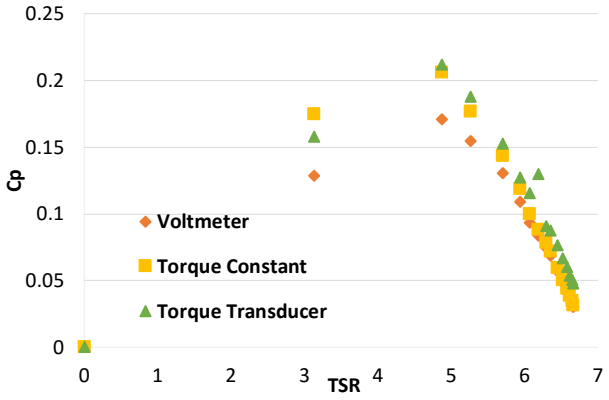

Figure 16. Coefficient of Power vs. Tip Speed Ratio at 5.59 (12.5 mph)

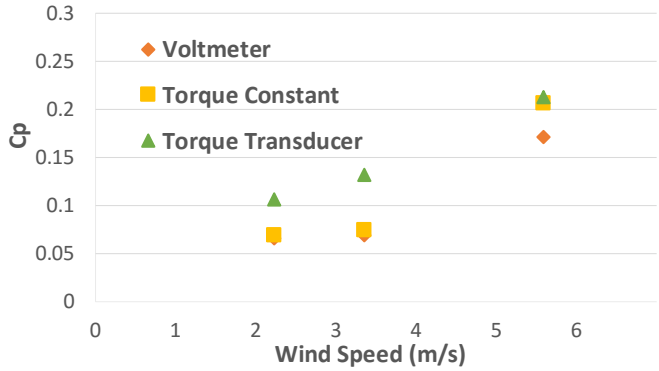

Figure 17. Coefficient of Power vs. Wind Speed

make the calculation of power with the torque constant is calculated from the voltage provided by the voltmeter. Again, taking into account the system losses, the calculated current can be lower, therefore, slightly lowering the C_P value when using the torque constant to calculate the coefficient of power. The torque transducer provides the highest C_p measurement because this value does not account for any of

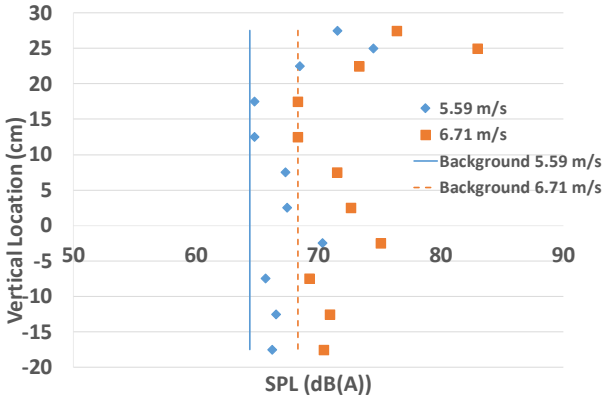

Figure 18. Vertical Location vs Corrected, A-Weighted Sound Pressure Level

the electrical system losses. This measurement is of the mechanical and aerodynamic power production of the wind turbine blades.

Figure 18 shows the vertical location versus the corrected, A-weighted Sound Pressure Level (SPL) for 5.59 and 6.71 m/s (12.5 and 15 mph). The A-weighted SPL is the sound measurement that is the more common as it closely matches the human ear. The vertical lines represent the tunnel background noise for each wind speed. The zero on the vertical axis is the center of the turbine hub. The main trend from this graph is that the noise increases at the tips, and then decreases when moving towards the hub. The tips create more noise, almost 83 dB (A) for the 6.71 m/s case, due to the high tip speeds and the vortices that this produces. The slower relative speeds down the span of the blade result in the lower noise signatures. Near the hub, the interactions with the spinner, the generator, and the transducers increases the noise. Once away from the hub, the SPL again drops to the lower levels. The slight increase below the hub is a result of the flow interacting with the wind turbine supporting post. The higher wind speeds at 6.71 m/s (15 mph) lead to the increase in noise generation, as expected. Tests at the lower wind speeds of 2.24, 3.35, and 4.47 m/s (5, 7.5, and 10 mph) did not produce meaningful SPL results. The background noise correction equation, Eq. 1, is no longer valid when the two noise measurements are within 3 dB(A). The noise produced by the turbine at the two lower wind speeds did not yield noise signatures that were noticeably different from the background noise in the tunnel. It is expected that the lower wind speeds will produce higher noise at the tips and the hub, and then lower noise signatures along the central parts of the blade as is seen with the higher wind speeds.

Lessons Learned

The development and testing of this wind turbine stand has proven to be very useful for testing of small-scale wind turbine blades. While the stand is functional, some challenges have arisen while testing. An unusually high percentage of humidity in the lab caused the brushes on the original generator to deteriorate. Two generators of the same model, one with a different type brush, were purchased so that a comparison could be made between the new test stand and previous data. One generator was a “precious metals” generator. This generator has brushes that are made from precious metals and therefore are unaffected by the moisture in the lab, making it a much more reliable generator for future tests. Both generators compared favourably to previous data.

Another concern that arose were vibrations of the test stand. With the cantilevered arm of the torque transducer, the generator and the turbine blades not being strongly supported, at natural harmonics, the test stand was subjected to noticeable vibrations. Moving past this harmonic vibration to higher speeds did show some minor vibrations of the test stand, but testing was still able to be completed. A new design for the generator housing is being explored.

For noise testing, the only concern was that at low speeds the wind tunnel background noise dominates the test measurement. Another wind tunnel, especially one with an open test section, may be quieter and, therefore, more suitable for these tests.

CONCLUSIONS

Wind energy continues to be an important source of renewable/sustainable energy and will be for years to come. Among renewable energies, wind energy is dominant and is currently responsible for 33% of all new renewable energy. Small-scale wind turbines hold promise especially in local or micro-grid applications. Urban wind turbines fall into this category. These wind turbines require a turbine optimization for maximum power production and are designed to also be quiet when sited in populated areas such as cities. To design and test such a small, urban wind turbine starts with the selection of the appropriate airfoil cross section which is then incorporated into a wind turbine blade design. Low Reynolds number flow aerodynamic data is necessary to accurately predict performance, however, this data is difficult to find and often needs to be experimentally determined. Knowing the lift and drag data allows the designer to find the optimum angle of attack for the design, the angle corresponding to the maximum lift to drag ratio. After designing the wind turbine blade for the local wind conditions, the next step is to use 3-D printing to manufacture the blades, hub, and spinner for the wind turbine rotor. Developing a model wind turbine system and experimental testing of the system in a small wind tunnel allows actual performance to be determined. Scaling up the model wind turbine for both geometry and Reynolds number then gives a more accurate prediction of performance optimized for the conditions found at the urban site.

Not to be ignored is the measurement of the noise produced by the wind turbine. Measuring the SPL of the wind turbine allows a comparison of noise levels with the desire to reduce the generated noise by selecting an appropriate airfoil and tip treatment. By studying different airfoils and tips in a wind tunnel setting, recommendations can be made concerning which combination reduces the noise generation to an acceptable level. With this process now in place, the next step will be a study of wind turbines designed with different airfoil sections and tip treatments. Comparisons can then be made for wind turbine blades that will lead to a wind turbine system designed to optimize performance and reduce the noise.

NOMENCLATURE

BEMT – Blade Element Momentum Theory
C_P – Coefficient of Power
HAWT – Horizontal Axis Wind Turbine
HVAC – Heating, Ventilation and Air Conditioning
MPP – Maximum Power Point
NREL – National Renewable Energy Laboratory
NAFNoise – NREL AirFoil Noise
SPL – Sound Pressure Level
TSR – Tip Speed Ratio
UAS – Unmanned Aerial System
VI – Virtual Instrument

REFERENCES

[1] World Population Prospects, The 2015 Revision: Key Findings and Advance Tables, United Nations, 2015

[2] Organisation for Economic Co-Operation and Development/International Energy Agency, World Energy Outlook 2015, Paris, France, November 2015.

[3] Energy Information Administration, 2016, "International Energy Outlook 2016," DOE/EIA-0484, U.S. Department of Energy, Washington DC.

[4] Global Wind Report: Annual Market Update 2015, Global Wind Energy Council, http://www.gwec.net/publications/global-wind-report-2/global-wind-report-2015-annual-market-update/ accessed on September 6, 2016.

[5] 2015 Small Wind World Report Summary, World Wind Energy Association, March 2015.

[6] American Wind Energy Association, Small Wind, http://www.awea.org/Issues/Content.aspx?ItemNumber=4592&navItemNumber=723, accessed on May 17, 2016.

[7] Renewable UK. Small and Medium Wind UK Market Report, October 2013.

[8] Clausen, P. D., and Wood, D. H., 1999, "Research and Development Issues for Small Wind Turbines," Renewable Energy, 16, pp. 922-927.

[9] Kishore, R. A., Coudron, T., and Priya, S., 2013, "Small-Scale Wind Energy Portable Turbine (SWEPT)," Journal of Wind Engineering and Industrial Aerodynamics, 116, pp. 21-31.

[10] Orrell, A. C., and Foster, N. F., 2015 Distributed Wind Market Report, U. S. Department of Energy, Richland, Washington, August 2016.

[11] Woolsey, R. J., Kleinfeld, R., and Sexton, Chelsa, 2010, "No Strings Attached: The Case for a Distributed Grid and a Low-Oil Future," World Affairs, 173 (3), pp. 59-71.

[12] Dodman, D., 2009, "Blaming Cities for Climate Change? An Analysis of Urban Greenhouse Gas Emissions Inventories," Environmental & Urbanization, Vol 21(1), pp. 185-201. DOI: 0.1177/0956247809103016.

[13] Torcellini, P., Pless, S., Deru, M., and Crawley, D., 2006, "Zero Energy Buildings: A Critical Look at the Definition," NREL/CP-550-39833.

[14] Grahm, P., 2014, "Integrating Renewable Energy Requirements in Building Codes Key to Helping the Building Sector Achieve its Mitigation Potential," Global Building Performance Network (GBPN), http://www.gbpn.org/our-blog/integrating-renewable-energy-requirements-building-codes-key-helping-building-sector , accessed on September 5, 2016.

[15] Aerotecture International Inc., http://www.aerotecture.com/products.html , accessed on September 5, 2016.

[16] Hong Kong Micro Wind Turbine Arrays, http://www.reuk.co.uk/index.htm, accessed on September 5, 2016.

[17] Dayan, E., 2006, "Wind Energy in Buildings: Power generation from wind in the urban environment – Where it is needed most," Refocus, 1471 0856/06, March/April 2006, pp 33 – 38.

[18] Millward-Hopkins, J. T., Tomlin, A. S., Ma, L., Ingham, D. B., and Pourkashanian, M., 2013, "Assessing the potential of urban wind energy in a major UK city using an analytical model," Renewable Energy, 60, pp 701-710.

[19] Booker, J. D., Mellor, P. H., Wrobel, R. and Drury, D., 2010, "A compact, high efficiency contra-rotating generator suitable for wind turbines in the urban environment," Renewable Energy, 35, pp 2027-2033.

[20] Lu, L., and Ip, K. Y., 2009, "Investigation on the feasibility and enhancement methods of wind power utilization in high-rise buildings in Hong Kong," Renewable and Sustainable Energy Reviews, 13, pp 450—461.

[21] Sunderland, K., Woolmington, T., Blackledge, J., and Conlon, M., 2013, "Small wind turbines in turbulent (urban) environments: A consideration of normal and Weibull distributions for power prediction" Journal of Wind Engineering and Industrial Aerodynamics, 121, pp 70-81.

[22] Duggan, C. D., and Jak, M. J. G., 2004, "Wind Power for Urban Applications," Proceedings of ASME Power 2004, March 30-April 1, 2004, Baltimore, Maryland.

[23] Walker, S. L., 2011, "Building mounted wind turbines and their suitability for the urban scale – A review of methods of estimating urban wind resource," Energy and Buildings, 43, pp 1852-1862.

[24] Drew, D. R., Barlow, J. F., and Cockerill, T. T., 2013, "Estimating the potential yield of small wind turbines in urban areas: A case study for Greater London, UK," Journal of Wind Engineering and Industrial Aerodynamics, 115, pp 104-111.

[25] Balduzzi, F., Bianchini, A., Carnevale, E. A., Ferrari, L., and Magnani, S., 2012, "Feasibility analysis of a Darrieus vertical-axis wind turbine installation in the rooftop of a building," Applied Energy, 97, pp 921-929.

[26] Abohela, I., Hamza, N., and Dudek, S., 2013, "Effect of roof shape, wind direction, building height and urban configuration on the energy yield and positioning of roof mounted wind turbines," Renewable Energy, 50, pp 1106-1108.

[27] Dursun, A., and Saglam, S., 2012, "A technical review of building-mounted wind power systems and a sample simulation model," Renewable and Sustainable Energy Reviews, 16, pp 1040-1049.

[28] Blanch, M.J., “Wind Energy Technologies for use in the Built Environment.” Wind Engineering, 26 (3), pp. 125-143, 2002.
[29] Simic, Z., Havelka, J. G., and Vrhovcak, M. B., 2013, “Small Wind Turbines – A unique segment of the wind power market,” Renewable Energy, 50, 1027 – 1036.
[30] Mithraratne, N., 2009, “Roof-top wind turbines for microgeneration in urban houses in New Zealand,” Energy and Buildings, 41, pp 1013- 1018.
[31] Brooks, T., Pope, D., and Marcolini, M., "Airfoil Self-Noise and Prediction," NASA Reference Publication 1218, National Aeronautics and Space Administration, 1989.
[32] Wagner, S., BareiB, R., and Guidati, G., 1996, Wind Turbine Noise, Springer, Berlin, Germany, Chap. 4, ISBN: 978-3-642-88712-3.
[33] NWTC Information Portal (NAFNoise), 2014, “NAFNoise,” NREL, https://nwtc.nrel.gov/NAFNoise (accessed May 10, 2015).
[34] Van Treuren, K. W., 2016, “Small Horizontal Axis Wind Turbines: Current Status and Future Challenges,” GT2016-57701, ASME IGTI Turbo Expo 2016, Seoul, Kore, June 13-17, 2016.
[35] Hays, A., and Van Treuren, K. W., 2016, “Study of Noise Generation Using the Eppler 387, NACA 0012, NACA 4412 and NREL S823,” ASEE Gulf Southwest Graduate Student Competition, Texas Christian University, March 7-8, 2016.
[36] Hays, A., and Van Treuren, K. W., 2016, “Study of Noise Generation Using the NACA 4412 and NREL S823 Airfoils,” AIAA Region IV Graduate Student Competition, University of Texas at Arlington, April 1-2, 2016.
[37] Wisniewski, C., Byerley, A., Heiser, W., Van Treuren, K. W., Liller, W. “The Influence of Airfoil Shape, Tip Geometry, Reynolds Number and Chord Length on Small Propeller Performance and Noise.” 33rd AIAA Applied Aerodynamics Conference, Dallas, TX, 2015.
[38] Goçmen, T., and Özerdem, B., 2012, “Airfoil Optimization for Noise Emission Problem and Aerodynamic Performance Criterion on Small Scale Wind Turbines,” Energy and Exergy Modelling of Advanced Energy Systems, 46 (1), pp. 62-71.
[39] Selig, M., “UIUC Airfoil Coordinates Data Base,” http://m-selig.ae.illinois.edu/ads/coord_database.html, accessed on September 6, 2016.
[40] Drela, M., XFOIL: Subsonic Airfoil Development System, http://web.mit.edu/drela/Public/web/xfoil/, accessed on May 18, 2016.
[41] Van Treuren, K. W., 2015, “Small-Scale Wind Turbine Testing in Wind Tunnels Under Low Reynolds Number Conditions,” Journal of Energy Resources Technology, 137, 051208-1 - 051208-11, DOI: 10.1115/1.4030617
[42] Burdett, T. A., Gregg, J., and Van Treuren, K. W., 2011, “An Examination of the Effect of Reynolds Number on Airfoil Performance,” ESFuelCell2011-54720, 5th International Conference on Energy Sustainability & 9th Fuel Cell Science, Engineering and Technology Conference, Washington, D. C., Aug 7-10, 2011.
[43] Burdett, T. A., 2012, "Aerodynamic Design Considerations for Small-Scale, Fixed-Pitch, Horizontal-Axis Wind Turbines Operating in Class 2 Winds," M.S. Thesis, Baylor University, Waco, TX.
[44] Liller, W. R., 2015, “The Design of Small Propellers Operating at Low Reynolds Numbers and Associated Experimental Evaluation,” M.S. Thesis, Baylor University, Waco, TX
[45] Burdett, T. A., Van Treuren, K. W., “Scaling Small-Scale Wind Turbines for Wind Tunnel Testing.” ASME Turbo Expo, Copenhagen, Denmark, June 11-15, 2012.
[46] Chen, T. Y., and Liou, L. R., 2011, “Blockage Corrections in Wind Tunnel Tests of Small Horizontal-Axis Wind Turbines,” Experimental Thermal and Fluid Sciences, 35, pp. 565-569.
[47] Kline, S. J., and F. A. McClintock: "Describing Uncertainties in Single-Sample Experiments", Mech. Eng., p. 3, January 1953
[48] Driscoll, D. P., “Noise, OSHA Technical Manual”, U.S. Department of Labor, https://www.osha.gov/dts/osta/otm/new_noise/, accessed on September 6, 2016.